

Further Improvement of Phosphite Dehydrogenase Thermostability by Saturation Mutagenesis

Michael J. McLachlan,¹ Tyler W. Johannes,² Huimin Zhao^{1,2}

¹Center for Biophysics and Computational Biology, University of Illinois at Urbana-Champaign, 600 South Mathews Avenue, Urbana, Illinois 61801; telephone: 217-333-2631; fax: 217-333-5052; e-mail: zhao5@uiuc.edu

²Department of Chemical and Biomolecular Engineering, University of Illinois at Urbana-Champaign, 600 South Mathews Avenue, Urbana, Illinois 61801

Received 25 March 2007; revision received 30 May 2007; accepted 11 June 2007

Published online 5 July 2007 in Wiley InterScience (www.interscience.wiley.com). DOI 10.1002/bit.21546

ABSTRACT: Phosphite dehydrogenase represents a new enzymatic system for regenerating reduced nicotinamide cofactors for industrial biocatalysis. We previously engineered a variant of phosphite dehydrogenase with relaxed cofactor specificity and significantly increased activity and stability. Here we performed one round of random mutagenesis followed by comprehensive saturation mutagenesis to further improve the enzyme thermostability while maintaining its activity. Two new thermostabilizing mutations were identified. These, along with the 12 mutations previously identified, were subjected to saturation mutagenesis using the parent enzyme or the engineered thermostable variant $12\times$ as a template, followed by screening of variants with increased thermostability. Of the 12 previously identified sites, 6 yielded new variants with improved stability over the parent enzyme. Several mutations were found to be context-dependent. On the basis of molecular modeling and biochemical analysis, various mechanisms of thermostabilization were identified. Combining the most thermostabilizing mutation at each site resulted in a variant that showed a 100-fold increase in half-life at 62°C over the $12\times$ mutant. The final mutant has improved the half-life of thermal inactivation at 45°C by 23,000-fold over the parent enzyme. The engineered phosphite dehydrogenase will be useful in NAD(P)H regeneration.

Biotechnol. Bioeng. 2008;99: 268–274.

© 2007 Wiley Periodicals, Inc.

KEYWORDS: thermostability; saturation mutagenesis; NAD(P)H regeneration; directed evolution

Introduction

Biocatalysts are an attractive alternative to chemical catalysts in industry for many reasons, including high substrate specificity, an ability to operate under mild environmental conditions, and production of stereo-specific products. Consequently, much research has been undertaken to develop enzyme-mediated reactions (Panke et al., 2004; Rubin-Pitel and Zhao, 2006). Enzymes such as oxidoreductases, however, often require cofactors such as NAD^+/NADH or $\text{NADP}^+/\text{NADPH}$ which are oxidized or reduced during the reaction. Cofactor regeneration is an important consideration for the economical use of such enzymes in industrial processes as they are too expensive to be added stoichiometrically (Zhao and van der Donk, 2003). One method that has found success is the coupling of the desired process to another enzyme reaction that converts the cofactor back to the required oxidation state (Wichmann and Vasic-Racki, 2005). The most widely used enzyme for this coupling is the formate dehydrogenase from *Candida boidinii* (Wichmann et al., 1981), which Degussa used to produce the amino acid derivative L-tert-leucine on the multi-ton scale (Tishkov and Popov, 2006).

However, the more recently discovered *Pseudomonas stutzeri* phosphite dehydrogenase (PTDH) that catalyzes NAD-dependent oxidation of phosphite into phosphate seems to have several advantages over the formate dehydrogenase (Costas et al., 2001; Johannes et al., 2007; Relyea and van der Donk, 2005). These advantages include an inexpensive sacrificial phosphite substrate, a benign phosphate product, and a favorable equilibrium constant. As natural enzymes are seldom optimal for use in industrial processes, PTDH has been engineered to improve its catalytic properties. Rational design based on a homology

Correspondence to: H. Zhao

Contract grant sponsor: National Science Foundation

Contract grant number: BES-0348107

Contract grant sponsor: Biotechnology Research and Development Consortium (BRDC)

Contract grant number: Project 2-4-121



model of PTDH led to mutagenesis of sites 175 and 176, allowing for much greater efficiency in the use of NADP as the nicotinamide cofactor (Woodyer et al., 2003). Directed evolution was applied to the wild-type PTDH to significantly increase the solubility and turnover number of the enzyme, and the resulting variant is referred to herein as the “parent” enzyme (Woodyer et al., 2006). Directed evolution was used to greatly enhance the parent enzyme thermostability, resulting in the 12× PTDH mutant that showed a more than 7,000-fold longer half-life of thermal inactivation than that of the parent PTDH at 45°C (Johannes et al., 2005).

Despite the drastic improvement in PTDH thermostability, it was believed that further improvement could be made due to the following reasons. The previous approach of screening libraries generated by error-prone PCR (Johannes et al., 2005) is capable of generating improved variants without the need for structural information, but is limited by the inability to access all possible amino acid substitutions at any given site. Thus, a saturation mutagenesis approach at thermostabilizing sites identified by error-prone PCR is advantageous. This approach was successfully used to enhance the thermal stability of other enzymes (Miyazaki and Arnold, 1999). As an added benefit, using this approach would also provide greater insight into the mechanism of thermal stabilization by analyzing multiple mutations at a particular site.

In this work we describe the saturation mutagenesis study of residues implicated in bestowing improved thermal stability to phosphite dehydrogenase. Of 12 previously identified sites, 6 yielded new variants with improved stability over the parent enzyme. Error-prone PCR and saturation mutagenesis generated thermostabilizing mutations at two additional sites. Some of the thermostabilizing mutations were context-dependent. Combination of the most thermostabilizing mutation at each site resulted in a variant that showed a 100-fold increase in half-life of thermal inactivation at 62°C over the 12× PTDH mutant. Possible mechanisms of thermostabilization are discussed on the basis of molecular modeling and biochemical analysis.

Materials and Methods

Saturation Mutagenesis

Overlap extension PCR was used to generate libraries of PTDH genes encoding all possible amino acids at sites 71, 130, 132, 137, 150, 215, 275, 276, 313, 315, 319, and 325. The parent construct was amplified as two fragments that overlapped around the site that was mutated. Fragment 1 used primers pRW2_For_NdeI (5'-TTT TTG GAT GGA GGA ATT CAT ATG-3') and a site-specific reverse primer. Fragment 2 used a site-specific forward primer and PTDH_Rev_PciI (5'-GTA CGT CGA TAC ATG TTT ATC AGT CTG CGG CAG G-3'). PCR was performed in

a volume of 50 μ L with cycle conditions of 94°C 4 min, (94°C 45 s, 55°C 45 s, 72°C 45 s) \times 25 cycles, 72°C 7 min. Fragments 1 and 2 were gel purified using QIAEX II Gel Extraction kit (Qiagen, Valencia, CA). The PCR products were digested with *DpnI* to remove the parent plasmid (3 h at 37°C with 10 U of *DpnI*), and purified with QIAquick PCR purification kit (QIAGEN). Fragments 1 and 2 (0.026 ng \times length in base pairs) were joined by overlap extension to create the full-length gene. A 20 μ L reaction with *PfuTurbo* DNA polymerase (Stratagene, La Jolla, CA) was cycled for 95°C for 2 min, 10 cycles of 94°C for 1 min, 55°C for 1 min, and 72°C for 3 min, with a final extension of 72°C for 10 min. Four microliters of this reaction mixture was used as a template for a 100 μ L PCR reaction using the primers pRW2_For_NdeI and PTDH_Rev_PciI. The reaction was purified with QIAEX II Gel Extraction kit (QIAGEN). The insert was digested with *NdeI* and *PciI* and ligated into the pRW2 vector. This library was electrotransformed into *E. coli* BW25141 competent cells.

Library Screening

A 96-well plate assay was used to screen for phosphite dehydrogenase activity, as previously described (Johannes et al., 2005). For screening in the parent genetic background, a temperature of 42°C was used, while 62°C was used for the libraries in the 12× PTDH mutant background.

Enzyme Purification

Selected mutants were cloned into pET15b as a *N*-terminal His-tagged construct and verified by DNA sequencing using the BigDyeTM Terminator sequencing method and an ABI PRISM 3700 sequencer (Applied Biosystems, Foster City, CA). Small-scale protein purification was carried out as described previously (Johannes et al., 2005). Glycerol was added to a concentration of 20% and the enzyme was stored at -80°C .

Thermostability and Optimal Temperature Determination

Purified enzyme was diluted to 0.2 mg/mL in 50 mM morpholinepropanesulfonic acid (MOPS) buffer (pH 7.25), incubated at 45°C, 50°C, or 62°C, and samples were removed at varying time points. Activity of each sample was measured by adding 10 μ L of enzyme to 490 μ L of 2 mM phosphite/1 mM NAD⁺ and the initial rate of increase in absorbance at 340 nm was monitored in a Cary 100 Bio UV-Visible spectrophotometer (Varian, Palo Alto, CA). The data were modeled with an exponential decay curve and the half-life determined from the exponential coefficient. The activity of improved enzyme variants was measured at temperatures between 20°C and 70°C in 5°C increments.

T_m Measurement by Circular Dichroism

To measure the melting temperature (T_m) of the enzyme variants, thermal denaturation was monitored by circular dichroism. Samples were prepared by adding 120 μg of protein to 50 mM potassium phosphate buffer (pH 7.0)/1 M urea in a final volume of 2 mL (1 M urea did not cause significant unfolding of the enzyme and was included to reduce protein aggregation during thermal denaturation). The sample was placed in a quartz cuvette with a 1 cm path-length and heated in a Peltier-controlled cell at a rate of 1°C per min. Ellipticity was monitored at 222 nm in a Jasco spectropolarimeter (Jasco Inc., Easton, MD). The midpoint of the denaturation curve was determined with Microcal Origin 5.0 software (OriginLab Corporation, Northampton, MA).

Enzyme Kinetics

Enzyme kinetics were determined at 25°C by measuring the activity of 3 μg enzyme when either NAD^+ or phosphite was held at 2 mM, and the other substrate was present at 5, 50, 100, 400, or 2,000 μM . The data were used to calculate the kinetic constants by fitting of the Michaelis–Menten equation using Microcal Origin 5.0 (OriginLab).

Results

Fourth Round of Screening for Thermostability

Error-prone PCR was performed on the 12 \times PTDH mutant, which had been generated by three previous rounds of error-prone PCR and high throughput screening (Johannes et al., 2005). This produced the variants 4-4G2 and 4-11C3. DNA sequencing revealed two new mutations, A146S and F198I. The mutation A146S was cloned into the parent PTDH template in pET15b, expressed, and purified. Note that the parent PTDH contained five mutations that increased solubility and activity: D13E, M26I, E175A, E332N, and C336D (Woodyer et al., 2006). Its thermostability was almost identical to that of the wild-type enzyme (Johannes et al., 2005). The A146S mutation was shown to increase the half-life of thermal inactivation at 45°C from around 1 min to 8 min (Table I). The F198I mutation led to low activity (data not shown) and was not cloned into the parent background.

Saturation Mutagenesis

Saturation mutagenesis was performed separately on each of the following residues in the parent PTDH template: V71, E130, Q132, Q137, I150, Q215, R275, L276, I313, V315, A319, and A325. Residues A146 and F198 were mutated in the context of the 12 \times PTDH mutant. The libraries were screened for increased thermostability at 45°C for the parent

Table I. Mutations identified from saturation mutagenesis and their half-lives of thermal inactivation and melting temperatures.

Site	Mutant	Mutation	$t_{1/2}$ (min, 45°C)	T_m (°C)
	Parent		1.07 \pm 0.07	39.7 \pm 0.3
71	V71I ^a	GTC \rightarrow ATC	1.30 \pm 0.11	40.3 \pm 0.1
101	T101A	ACG \rightarrow GCG	4.52 \pm 0.66	41.1 \pm 1.6
130	E130Q	GAG \rightarrow CAG	7.43 \pm 0.25	47.0 \pm 4.6
130	E130R	GAG \rightarrow CGG	9.30 \pm 0.43	46.1 \pm 1.6
130	E130K ^a	GAG \rightarrow AAG	12.56 \pm 0.35	47.3 \pm 2.0
132	Q132K	CAG \rightarrow AAG	2.76 \pm 0.01	41.5 \pm 2.5
132	Q132R ^a	CAG \rightarrow CGG	2.30 \pm 0.01	39.0 \pm 3.5
137	Q137H	CAG \rightarrow CAT	4.62 \pm 0.80	42.7 \pm 1.0
137	Q137R ^a	CAG \rightarrow CGG	3.90 \pm 0.14	42.7 \pm 2.4
146	A146S	GCT \rightarrow TCC	8.23 \pm 0.49	41.2 \pm 1.6
150	I150F ^a	ATC \rightarrow TTC	7.00 \pm 1.60	42.0 \pm 0.6
198	F198M	TTC \rightarrow ATG	2.15 \pm 0.13	40.6 \pm 1.4
215	Q215M	CAG \rightarrow ATG	2.46 \pm 0.15	40.8 \pm 1.4
215	Q215L ^a	CAG \rightarrow CTG	8.70 \pm 0.80	40.9 \pm 1.8
275	R275L	CGG \rightarrow CTC	9.09 \pm 0.40	41.6 \pm 0.6
275	R275Q ^a	CGG \rightarrow CAG	4.60 \pm 0.40	40.0 \pm 1.0
276	L276C	CTG \rightarrow TGC	11.72 \pm 0.18	44.7 \pm 1.0
276	L276H	CTG \rightarrow CAC	2.05 \pm 0.3	40.5 \pm 0.4
276	L276R	CTG \rightarrow CGG	7.76 \pm 0.71	43.6 \pm 2.4
276	L276Q ^a	CTG \rightarrow CAG	3.58 \pm 0.23	41.4 \pm 0.3
276	L276S	CTG \rightarrow TCC	3.29 \pm 0.04	39.8 \pm 0.6
313	I313L ^a	ATC \rightarrow CTC	1.05 \pm 0.03	39.2 \pm 0.3
315	V315A ^a	GTA \rightarrow GCA	1.14 \pm 0.11	40.7 \pm 0.7
	A319E/T101A	GCG \rightarrow GAG	5.34 \pm 0.35	41.9 \pm 0.1
		ACG \rightarrow GCG		
319	A319E ^a	GCG \rightarrow GAG	2.14 \pm 0.06	40.6 \pm 0.6
325	A325V ^a	GCG \rightarrow GTG	1.01 \pm 0.03	39.3 \pm 0.1

^aThese mutations are original mutations found in the 12 \times mutant.

PTDH template or 62°C for the 12 \times PTDH template, and promising variants were selected for further analysis. Variants that showed increased stability were sequenced to identify the mutations. These variants were sub-cloned into the vector pET15b followed by protein purification for characterization. Table I shows the half-lives of thermal inactivation of the mutant proteins in the parent template when incubated at 45°C. Apart from the mutations known from error-prone PCR of this protein (Johannes et al., 2005), no additional substitutions conferring increased stability were found for residues V71, A146, I150, I313, V315, A319, or A325. For residue E130, glutamine and arginine substitutions increased stability substantially. A lysine substitution at residue Q132 showed slightly higher stability than that of the known arginine substitution, as did a histidine substitution at residue Q137 compared to the arginine substitution. The methionine substitution increased the stability when present at residue F198, without decreasing activity. Methionine substituted at residue Q215 gave a moderate increase to stability but to a lesser extent than the known leucine mutation. An arginine to leucine substitution at residue R275 greatly increased stability. Many new beneficial mutations were seen at residue L276, namely histidine, serine, arginine, and cysteine.

During screening of the residue A319 saturation library, a spontaneous threonine to alanine mutation was observed at

position 101. When T101A was introduced separately into the parent enzyme, it conferred a fourfold increase in stability. In the context of the 12× PTDH variant, however, this mutation led to a decrease in stability (data not shown).

Generation of Optimized Thermostable Variants

The most thermostabilizing mutation discovered for each particular site was incorporated into the 12× PTDH mutant. This was performed for K132, H137, L275, and C276, forming an optimized thermally stable phosphite dehydrogenase termed Opt12. The addition of A146S to Opt12 led to the Opt13 variant, and the further addition of F198M led to Opt14, the final mutant showing 14 amino acid substitutions from the parent enzyme, and 19 amino acid substitutions from the wild-type enzyme.

Characterization of Mutants

The half-lives of thermal inactivation at 45°C for enzymes containing single mutations in the parent background are displayed in Table I. The parent enzyme has a half-life at this temperature of around 1 min. The best single mutations increase this by over 10-fold. Interestingly, some of the mutations previously found did not show significant increases in half-life of thermal inactivation when introduced individually into the parent enzyme, namely I313L, V315A, A325V, and to a lesser extent V71I. These were all found in the second and third rounds of error-prone PCR (Johannes et al., 2005). Table II shows the half-lives of thermal inactivation of the optimal mutants at 45°C, 50°C, and 62°C. By using the best mutations at each of the 12 initial sites, improvements in half-life over the 12× mutant were seen by 1.5-, 2.7-, and 8.8-fold at 45, 50, and 62°C, respectively. The addition of thermostabilizing mutations at sites 146 and 198 led to a dramatic increase in stability at 62°C, with notable improvements at lower temperatures. The Opt14 mutant had a half-life of 450 min at 62°C, increased over 100-fold from the 12× mutant. At 45°C, the half-life of thermal inactivation of the Opt14 mutant was approximately doubled compared to that of the 12× mutant, representing over 23,000-fold improvement compared to the parent enzyme.

The apparent melting temperatures of all the PTDH mutants were determined by circular dichroism. Unfolding

Table II. Thermal stability of optimal mutants.

Enzyme	$t_{1/2}$ (min, 45°C)	$t_{1/2}$ (min, 50°C)	$t_{1/2}$ (min, 62°C)	T_m (°C)
Parent	1.07 ± 0.07	nd	nd	39.7 ± 0.3
12×	13246 ± 3289	3868 ± 355	4.0 ± 0.8	59.7 ± 1.0
Opt12	20441 ± 7536	10331 ± 1757	35 ± 1.2	63.9 ± 1.3
Opt13	24875 ± 3770	14757 ± 1129	210 ± 21	64.2 ± 1.1
Opt14	25518 ± 2144	15415 ± 1049	450 ± 49	64.4 ± 0.8

nd = not determined.

was seen to be irreversible, and the midpoints of the denaturation curves representing the melting temperature T_m are reported in Tables I and II. The T_m of the parent enzyme was just under 40°C, with single mutations having effects ranging from very little up to increasing T_m by 7°C. The 12× mutant had a T_m of around 60°C, and the three improved variants, Opt12, Opt13, and Opt14, were around 64°C.

The optimal temperature of the stabilized enzymes was examined by measuring the initial activity at temperatures ranging from 20°C to 70°C, and is shown in Figure 1. The parent phosphite dehydrogenase has an optimal temperature of around 40°C. The 12×, Opt12, and Opt13 mutants have an optimal temperature around 50°C, with the Opt14 optimum decreasing to 45°C. The activities of the Opt12 and Opt13 mutants were higher than those of the 12× mutant and the parent enzyme, while the Opt14 had activities lower than the 12× mutant at temperatures above 45°C.

The improved mutants from this work were subjected to kinetic analysis at 25°C with respect to NAD^+ and phosphite (Table III). The Opt12 and Opt13 variants showed similar kinetics with a k_{cat} slightly higher than the 12× mutant but lower than the parent. The K_{M,NAD^+} for Opt12 and Opt13 was intermediate between the parent and the 12× mutant, while the K_M for phosphite $K_{M,Phosphite}$ was higher than both. The corresponding values of $k_{cat}/K_{M,NAD^+}$ of 4.3 and 4.0 $\mu\text{M}^{-1} \text{min}^{-1}$ for Op12 and Opt13, respectively, were similar to the parent, but lower than that of the 12× mutant (4.9 $\mu\text{M}^{-1} \text{min}^{-1}$). The Opt14 mutant showed a similar k_{cat} but a doubled K_{M,NAD^+} and tripled $K_{M,Phosphite}$ relative to the 12× mutant, which led to a reduction in k_{cat}/K_M .

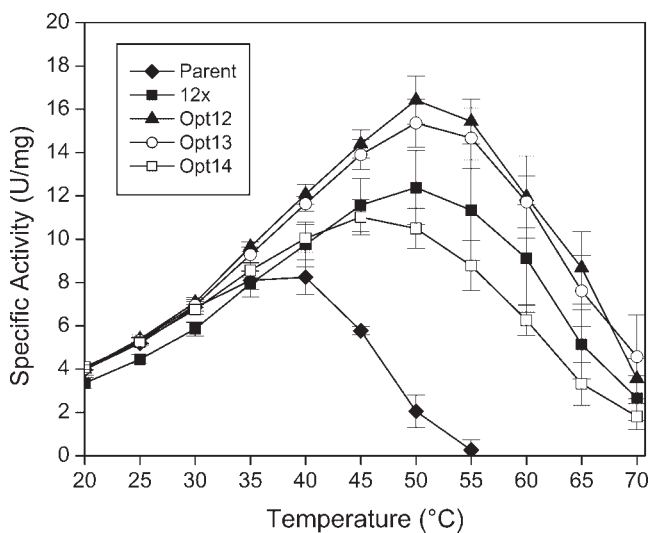


Figure 1. Specific activity (μmol NADH production per min per mg PTDH) of Parent, 12×, Opt12, Opt13, and Opt14 PTDH variants over a temperature range of 20°C–70°C.

Table III. Enzyme kinetics for the thermostable mutants.

Enzyme	k_{cat} (min^{-1})	K_M (μM , NAD ⁺)	K_M (μM , phosphite)	$k_{\text{cat}}/K_{M,\text{NAD}}$ ($\mu\text{M}^{-1}\text{min}^{-1}$)
Parent	262 ± 7	66 ± 7	57 ± 4	4.0
12×	195 ± 4	40 ± 3	46 ± 6	4.9
Opt12	213 ± 3	50 ± 5	79 ± 15	4.3
Opt13	213 ± 3	54 ± 6	90 ± 17	4.0
Opt14	219 ± 5	105 ± 15	142 ± 28	2.1

Discussion

Effectiveness of Saturation Mutagenesis

This work successfully demonstrated the usefulness of including saturation mutagenesis in a directed evolution strategy by further improving the stability of phosphite dehydrogenase by 100-fold at 62°C. The thermostability of the 12× phosphite dehydrogenase was improved by altering the amino acid at sites previously identified by error-prone PCR to be involved in stability. At 8 of the 12 original sites, no better mutations were discovered, but for sites 132, 137, 275, and 276, new thermostabilizing amino acid substitutions were revealed. The results showed that the thermostabilizing sites were not equally conducive to modification, with residue L276 showing five substitutions that were more stable, whereas residues such as V71 or I150 yielded no other thermostabilizing mutations. The number of base changes found was one for Q132K, one for Q137H, two for A146S, two for F198M, two for R275L (although the minimum needed was one), and three for L276C. Saturation mutagenesis thus focused screening at the examined sites, allowing all amino acids to be screened for their effect at these positions. Error-prone PCR produces a biased library of mutations since changes to multiple nucleotides in a codon are unlikely with this method, but multiple changes are necessary for some amino acid substitutions.

Saturation mutagenesis has been used very successfully in other cases to increase protein stability. At the extreme, every residue of a haloalkane dehalogenase gene was subjected to saturation mutagenesis, identifying eight substitutions that when combined resulted in a 30,000-fold improvement in stability (Gray et al., 2001). The approach described in the current work is more manageable for most labs, consisting of an initial random mutagenesis screen followed by site-directed saturation mutagenesis, and has also been used successfully (Miyazaki and Arnold, 1999; Miyazaki et al., 2006; Wunderlich and Schmid, 2006).

Properties of the Best Mutants: Opt13 Versus Opt14

This work resulted in two improved mutants, Opt13 and Opt14 that showed a trade-off between activity and stability. The most thermally stable variant was Opt14, as indicated by the twofold increase in half-life at 62°C. However at 25°C, the k_{cat}/K_M indicates that Opt13 is the more efficient

enzyme, and from Figure 1 it can be seen that Opt13 shows a higher activity at elevated temperatures. The choice of the best variant to use may depend on the conditions of the reaction.

The decrease in optimal reaction temperature for Opt14 was unexpected. Typically, an increase in stability would be accompanied by an increase rather than a decrease in temperature optimum. Such effects have, however, been seen before and illustrate that thermostability and thermoactivity are distinguishable features of an enzyme. For instance, alteration of a loop region in citrate synthase from *Arthrobacter* resulted in a mutant 1.7-fold more stable at 45°C, but with an optimal temperature 5–6°C lower than the wild-type enzyme (Gerike et al., 2001). It has been proposed that such an effect may be explained by a model of inactivation involving equilibrium between active and inactive forms of an enzyme influenced by a temperature-dependent property K_{eq} , with the inactive enzyme form susceptible to irreversible thermal denaturation (Daniel et al., 2001).

Structural Basis for Stabilization

Protein stability is influenced by multiple factors (Sternier and Liebl, 2001; Vieille and Zeikus, 2001) including hydrogen-bonding networks, hydrophobic interactions, entropic effects, packing efficiency, multimerization, and amino acid composition. Mutations can be introduced to exploit these factors, however, there is no general method one can use to predict which changes should be made to increase the stability of a given protein. Rational approaches can be attempted (Eijsink et al., 2004), or one can use random mutagenesis and screening in a directed evolution strategy (Eijsink et al., 2004; Zhao and Arnold, 1999). By incorporating saturation mutagenesis here, we hoped to gain further insights into how the sites modified in the 12× mutant influenced stability. All the thermostabilizing mutations were mapped into a homology model of PTDH that we built previously (Johannes et al., 2005) (Fig. 2).

For the buried residues V71 and I150, no other stabilizing mutations were observed, and the mechanism of thermostabilization at these sites is still expected to be related to hydrophobic interactions (Johannes et al., 2005). Residues I313 and V315 are within an alpha helix and no further mutations were found for these sites, but both mutations were to a residue with higher helical propensity. We suspect

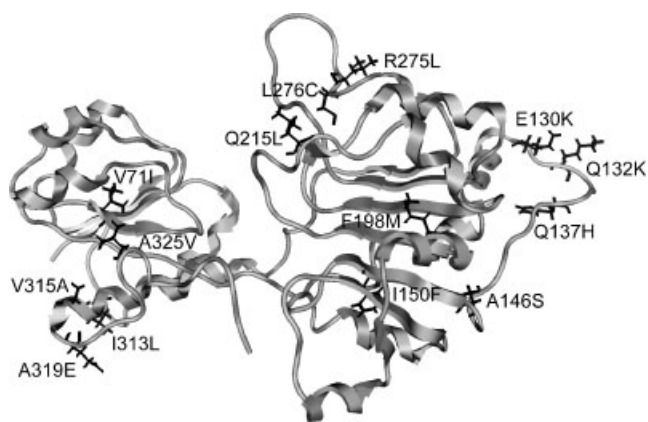


Figure 2. Homology model of the Opt14 mutant of phosphite dehydrogenase. The 14 residues involved in improving thermal stability are shown.

these mutations influence stability by the mechanism of alpha helix stabilization as proposed in our previous work (Johannes et al., 2005). Residues A319 and A325 are in an unstructured region near the C-terminus and may help anchor this region. The A319E mutation allows for hydrogen bonding between the carboxyl of glutamate and the amino group of glutamine 314. Residue Q215 is surface exposed, but when mutated from the hydrophilic glutamine residue to either leucine or methionine, both more hydrophobic, the stability is increased. This likely indicates that hydrophobic interactions with surrounding amino acids are generated by these mutations.

Residues E130, Q132, and Q137 are in the loop between $\alpha 6/\beta 5$, close to residues R275 and L276 on the other subunit of the dimer, and interactions involving some of these sites may contribute to dimer stabilization. When the negatively charged E130 was replaced by the positively charged lysine or arginine, or the neutral glutamine, a more stable enzyme was produced. This along with the negatively charged residues close to E130 on the other subunit (E264, E266, D267, and D272) would support a mechanism of balancing charge in the area. The enzyme was more stable when Q132 was replaced by the positively charged lysine or arginine, and when Q137 was replaced by positive arginine or the neutral/positive histidine. Some degree of the stabilization may arise due to the removal of glutamine 132/137 since the residue can lead to protein denaturation by deamidation, especially when the next residue is small such as G133 (Vieille and Zeikus, 2001). Mutagenesis of R275 showed that leucine stabilizes the enzyme better than the previously found glutamine mutation, both of which are neutral residues which may influence the charge distribution in the area beneficially. The many stabilizing mutations at residue L276 are polar or positively charged and more hydrophilic than the parent leucine. They may introduce hydrogen bonds with water molecules or other residues to increase the stability.

Residue A146 is positioned at the beginning of $\beta 5$ after an unstructured region, with backbone hydrogen bonds between its carboxyl group and the amino group of T170, and its amino and the carboxyl group of L143. Replacing the alanine with a serine would preserve these bonds but also allow the serine hydroxyl to form a hydrogen bond with the backbone of G142 or L143, thus helping to anchor the unstructured region. The final mutation, F198M, is situated on an alpha helix in a hydrophobic area formed by a beta sheet. Methionine is more stabilizing to an alpha helix than phenylalanine, and while being less hydrophobic, it is more flexible which may allow it to fill the space better.

The majority of the mutations seemed to have an additive effect, however there were exceptions. When introduced separately the mutations I313L, V315A, and A325V were not stabilizing in the parent sequence. No direct interactions were observed for these mutations to explain why they were stable in one context but not another. A non-additive effect was seen previously for Q132R when it was added to the 4 \times mutant containing Q137R, R275Q, Q215L, and I150F (Johannes et al., 2005).

In conclusion, this work has shown the benefit of applying saturation mutagenesis to improve protein stability and to decipher the mechanisms of thermal stabilization. By accessing all possible amino acids at these thermostabilizing sites, several mutations were found to increase the stability beyond those initially identified. The further engineering of the 12 \times mutant resulted in two PTDH variants, Opt13 and Opt14, with significantly enhanced stability at high temperatures without compromising turnover numbers, which should be useful for cofactor regeneration applications.

References

- Costas AM, White AK, Metcalf WW. 2001. Purification and characterization of a novel phosphorus-oxidizing enzyme from *Pseudomonas stutzeri* WM88. *J Biol Chem* 276:17429–17436.
- Daniel RM, Danson MJ, Eisenthal R. 2001. The temperature optima of enzymes: A new perspective on an old phenomenon. *Trends Biochem Sci* 26:223–225.
- Eijssink VG, Bjork A, Gaseidnes S, Sirevag R, Synstad B, van den Burg B, Vriend G. 2004. Rational engineering of enzyme stability. *J Biotechnol* 113:105–120.
- Gerike U, Danson MJ, Hough DW. 2001. Cold-active citrate synthase: Mutagenesis of active-site residues. *Protein Eng* 14:655–661.
- Gray KA, Richardson TH, Kretz K, Short JM, Bartnek F, Knowles R, Kan L, Swanson PE, Robertson DE. 2001. Rapid evolution of reversible denaturation and elevated melting temperature in a microbial haloalkane dehalogenase. *Adv Synth Catal* 343:607–617.
- Johannes TW, Woodyer RD, Zhao HM. 2005. Directed evolution of a thermostable phosphite dehydrogenase for NAD(P)H regeneration. *Appl Environ Microb* 71:5728–5734.
- Johannes TW, Woodyer RD, Zhao HM. 2007. Efficient regeneration of NADPH using an engineered phosphite dehydrogenase. *Biotechnol Bioeng* 96:18–26.
- Miyazaki K, Arnold FH. 1999. Exploring nonnatural evolutionary pathways by saturation mutagenesis: rapid improvement of protein function. *J Mol Evol* 49:716–720.

- Miyazaki K, Takenouchi M, Kondo H, Noro N, Suzuki M, Tsuda S. 2006. Thermal stabilization of *Bacillus subtilis* family-11 xylanase by directed evolution. *J Biol Chem* 281:10236–10242.
- Panke S, Held M, Wubbolts M. 2004. Trends and innovations in industrial biocatalysis for the production of fine chemicals. *Curr Opin Biotechnol* 15:272–279.
- Relyea HA, van der Donk WA. 2005. Mechanism and applications of phosphite dehydrogenase. *Bioorg Chem* 33:171–189.
- Rubin-Pitel SB, Zhao HM. 2006. Recent advances in biocatalysis by directed enzyme evolution. *Comb Chem High Throughput Screen* 9:247–257.
- Sternier R, Liebl W. 2001. Thermophilic adaptation of proteins. *Crit Rev Biochem Mol Biol* 36(1):39–106.
- Tishkov VI, Popov VO. 2006. Protein engineering of formate dehydrogenase. *Biomol Eng* 23:89–110.
- Vieille C, Zeikus GJ. 2001. Hyperthermophilic enzymes: Sources, uses, and molecular mechanisms for thermostability. *Microbiol Mol Biol Rev* 65:1–43.
- Wichmann R, Vasic-Racki D. 2005. Cofactor regeneration at the lab scale. *Adv Biochem Eng Biotechnol* 92:225–260.
- Wichmann R, Wandrey C, Buckmann AF, Kula MR. 1981. Continuous enzymatic transformation in an enzyme membrane reactor with simultaneous NAD(H) regeneration. *Biotechnol Bioeng* 67:791–804.
- Woodyer R, van der Donk WA, Zhao HM. 2003. Relaxing the nicotinamide cofactor specificity of phosphite dehydrogenase by rational design. *Biochemistry* 42:11604–11614.
- Woodyer R, van der Donk WA, Zhao HM. 2006. Optimizing a biocatalyst for improved NAD(P)H regeneration: Directed evolution of phosphite dehydrogenase. *Comb Chem High Throughput Screen* 9: 237–245.
- Wunderlich M, Schmid FX. 2006. *In vitro* evolution of a hyperstable G beta 1 variant. *J Mol Biol* 363:545–557.
- Zhao HM, Arnold FH. 1999. Directed evolution converts subtilisin E into a functional equivalent of thermitase. *Protein Eng* 12:47–53.
- Zhao HM, van der Donk WA. 2003. Regeneration of cofactors for use in biocatalysis. *Curr Opin Biotechnol* 14:583–589.